

G. SIWIEC*

ELIMINATION OF ALUMINUM DURING THE PROCESS OF Ti-6Al-4V ALLOY, SMELTING IN A VACUUM INDUCTION FURNACE

ELIMINACJA ALUMINIUM W PROCESIE WYTOPU STOPU Ti-6Al-4V W INDUKCYJNYM PIECU PRÓŻNIOWYM

In the paper, results of the study on kinetics of aluminum evaporation from a liquid Ti-6Al-4V alloy during its smelting in a vacuum induction furnace are presented. The experiments were performed with the use of a VIM 20-50 furnace (manufactured by SECO-WARWICK) at 1773 K and 5-1000 Pa. Based on the values of changes in aluminum concentration in a liquid alloy, overall mass transfer coefficients were estimated. Within the analysed pressure range, the coefficient values changed from $0.97 \cdot 10^{-5} \text{ ms}^{-1}$ to $1.93 \cdot 10^{-5} \text{ ms}^{-1}$ for 1000 Pa and 5 Pa, respectively.

Keywords: Vacuum Induction Melting, Ti-6Al-4V alloy, evaporation, mass transfer coefficient

W pracy przedstawiono wyniki badań kinetyki procesu odparowania aluminium z ciekłego stopu Ti-6Al-4V w trakcie jego wytopu w próżniowy piecu indukcyjnym. Badania realizowano w piecu VIM 20-50 produkcji firmy SECO-WARWICK w temperaturze 1773 K i zakresie ciśnień 5-1000 Pa. Na podstawie uzyskanych wyników zmian stężenia aluminium w ciekłym stopie oszacowano wartości ogólnego współczynnika transportu masy. W analizowanym zakresie ciśnień wartość tego współczynnika zmieniała się odpowiednio od $0,97 \cdot 10^{-5} \text{ ms}^{-1}$ dla ciśnienia 1000 Pa do $1,93 \cdot 10^{-5} \text{ ms}^{-1}$ dla ciśnienia 5 Pa.

1. Introduction

Evaporation of volatile metal bath components is strictly related to a lot of metal smelting, refining and casting processes. If any impurity is removed during evaporation, the process can be considered beneficial in terms of the metal product purity. However, when it involves a basic alloy component or microadditives, the process is unfavourable for a specialist in technology and metallurgy, so it should be limited. A sample technology involving evaporation of a basic bath component is Ti-Al-X alloy smelting which results in high aluminum content reduction during alloy treatment – either vacuum induction melting (VIM) or electron beam melting (EBM). In terms of kinetics, evaporation itself

is a complex process. Its rate is affected by temperature and pressure as well as e.g. alloy composition [1, 3] and hydrodynamic conditions in the melting device. In the last case, for alloy smelting in induction furnaces, it can be e.g. operating frequency or a position of the melting pot in relation to the inductor [4-6]. Another relevant factor is the effect of gaseous atmosphere on the process rate. It is particularly important for processes performed at the atmospheric pressure.

2. Research methodology

A Ti-6Al-4V alloy was investigated. Its composition is presented in Table 1.

TABLE 1

Chemical composition of the alloy used in the study

The content of the basic alloying elements, wt. %											
Ti	Al	V	Cr	Cu	Fe	Mo	Mn	Sn	Si	Zr	Pd
90.36	5.50	3.77	<0.02	<0.01	0.08	0.12	<0.01	<0.02	0.07	0.02	0.02

* SILESIAN UNIVERSITY OF TECHNOLOGY, DEPARTMENT OF METALLURGY, 40-019 KATOWICE, 8 KRASIŃSKIEGO STR., POLAND

Smelting experiments were performed with the use of a VIM 20-50 vacuum induction furnace manufactured by SECO-WARWICK. The device is equipped with, among others, an inductor tilt electric drive, a control panel for managing the process and adjusting its parameters, an alloy additive-feeding system, a sampling mechanism and, additionally, an ingot mould heating system. Basic parameters of the VIM 20-50 furnace are listed in Table 2.

TABLE 2

Basic parameters of the VIM 20-50 furnace

Furnace parameter	Parameter value
Maximum power rating	75 kW
Maximum vacuum	0.01 Pa
Pumping system	mechanical pump, Roots rotary pump, diffusion pump
Maximum operating temperature	2073 K
Maximum melting pot capacity	20 kg
Maximum ingot mould temperature	1123 K

During the experiment, a 1 kg alloy sample was placed in the graphite melting pot (inner diameter: 0.09 m; operating height: 0.22 m) mounted inside the furnace coil. After closing the furnace chamber, required pressure was generated by cooperating pumps: the mechanical, Roots and diffusion pumps. When the assumed level of vacuum was reached, the charge material was heated up to the set temperature and held for 600 s. For temperature measurements, a pyrometer and a PtRh-Pt ther-

mocouple were used. During the experiment, the liquid metal samples were collected and analysed with the use of a Foundry-Master Compact 01L00113 optical emission spectrometer. When the test was completed, liquid metal was poured into the graphite ingot mould. When it solidified and the furnace cooled down, the furnace chamber was opened. The metal cast was also subjected to the chemical analysis.

The experiments were performed at 1973 K and 5-1000 Pa.

3. Test results

Based on the values of aluminium concentration determined for the tested alloy samples, a change of that concentration during the smelting process was correlated by the following logarithmic function:

$$-\log \frac{C_{Al}^t}{C_{Al}^0} = A \cdot t \quad (1)$$

where: t – time, s,

C_{Al}^t – aluminum concentration in the alloy after time t , wt.%,

C_{Al}^0 – initial aluminum concentration, wt.%,

A – constant, s^{-1} .

In Table 3, “ A ” values from the equation (1), determined for all the experiments, are presented. Also, basic experimental parameters, final concentrations of aluminum in the alloy and its loss fractions are listed. A graphic representation of sample test results is shown in Fig. 1.

TABLE 3

Test results with regard to aluminum concentration changes in the Ti-6Al-4V alloy

Experiment no.	Pressure in the system, Pa	Final Al concentration in the alloy, % wt.	Constant A in equation (1), s^{-1}	Aluminum loss, %
1	1000	4,707	$1,22 \cdot 10^{-4}$	14,41
2	1000	4,720	$1,10 \cdot 10^{-4}$	14,18
3	100	4,370	$1,75 \cdot 10^{-4}$	20,54
4	100	4,380	$1,70 \cdot 10^{-4}$	20,36
5	50	4,307	$1,75 \cdot 10^{-4}$	21,69
6	50	4,200	$1,99 \cdot 10^{-4}$	23,63
7	10	4,220	$2,02 \cdot 10^{-4}$	23,27
8	10	4,170	$2,07 \cdot 10^{-4}$	24,18
9	5	4,063	$2,13 \cdot 10^{-4}$	26,12
10	5	4,080	$2,20 \cdot 10^{-4}$	25,81

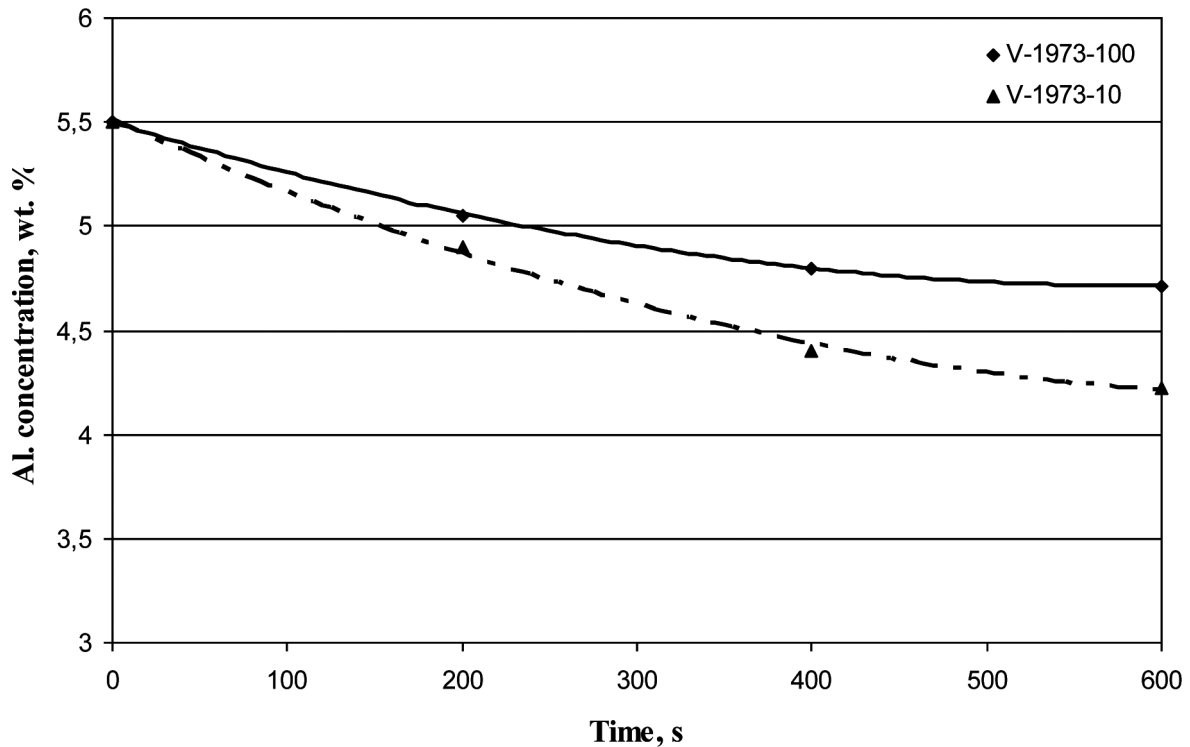


Fig. 1. Aluminum concentration changes during Ti-6Al-4V melting at 1973 K and 10 Pa (experiment no. 7), 1000 Pa (experiment no. 1)

4. Kinetics of evaporation

In the process of liquid metal alloy component evaporation, the following three main stages are distinguished:

- Transfer of the evaporating component from the body of the liquid metallic phase to the interface (in the investigated process: aluminum transfer from the Ti-Al-V alloy body to its surface) – stage I.
- Surface reaction, i.e. the evaporation process at the liquid metal – gaseous phase interface – stage II.
- Transfer of the evaporating component vapours from the interface to the core of gaseous phase (transfer of gaseous aluminum into the gaseous phase) – stage III.

A diagram of evaporation stages is presented in Fig. 2.

The overall flux of aluminum mass being transferred from the liquid titanium body to the gaseous phase can be described with the following relation [7]:

$$S_{Al} = \left(\frac{1}{\beta_{Al}^l} + \frac{1}{\beta_{Al}^g} + \frac{1}{k_{Al}^e} \right) \cdot C_{Al}^l \quad (2)$$

or

$$S_{Al} = k_{Al} \cdot C_{Al}^l \quad (3)$$

where: k_{Al} – overall aluminum mass transfer coefficient,
 β_{Al}^l – aluminum mass transfer coefficient in the liquid phase (titanium bath),

k_{Al}^e – aluminum evaporation rate constant,
 β_{Al}^g – aluminum mass transfer coefficient in the gaseous phase.

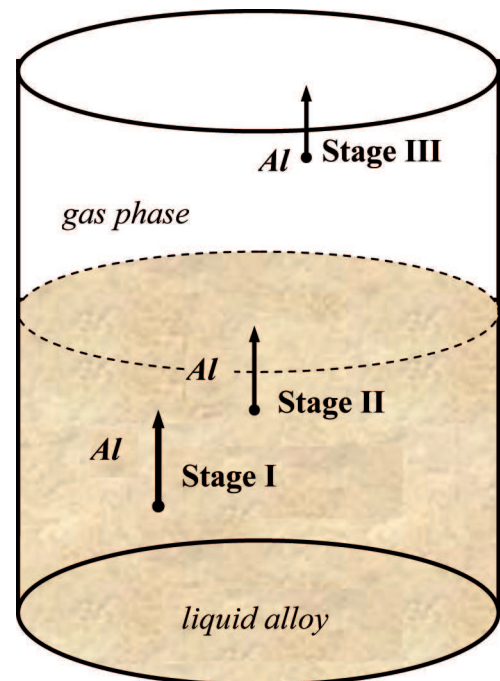


Fig. 2. Diagram of metal bath component evaporation stages

The k_{Al} is described with the following equation [7]:

$$\frac{1}{k_{Al}} = \frac{1}{\beta_{Al}^l} + \frac{1}{\phi k_{Al}^e} + \frac{RT}{\beta_{Al}^g \phi} \quad (4)$$

where:

$$\phi = \frac{p_{Al}^o \cdot \gamma_{Al} M_{Ti}}{\rho_{Ti}} \quad (5)$$

and: p_{Al}^o – equilibrium pressure of Al over pure bath,
 γ_{Al} – coefficient of Al activity in the liquid Ti-Al-X alloy,

M_{Ti} – titanium molar mass,

ρ_{Ti} – liquid titanium density.

T – temperature,

R – gas constant.

In order to determine the overall aluminum mass transfer coefficient from the experimental data, the process rate was described with the following equation:

$$\frac{dC_{Al}}{dt} = k_{Al} \cdot \frac{F}{V} \cdot C_{Al} \quad (6)$$

which assumed the following notation in the integral form:

$$\int_0^t \frac{dC_{Al}}{C_{Al}} = -k_{Al} \cdot \frac{F}{V} \int_0^t dt \quad (7)$$

Having integrated this relation, the following is obtained:

$$2,303 \log \frac{C_{Al}^t}{C_{Al}^o} = -k_{Al} \cdot \frac{F}{V} (t - t_o) \quad (8)$$

where: F – evaporation areas (interface),

V – liquid metal volume,

$(t - t_o)$ – process duration.

Knowing the value of constant A from equation (1) and using the relation (8), overall mass transport coefficients for the analysed process were determined. They are listed in Table 4.

In order to establish the fraction of mass transfer resistance in the liquid phase with regard to the overall process resistance, the values of mass transport coefficient β_{Al}^l were also estimated with the use of the following Machlin relation [8]:

$$\beta_l = \left(\frac{8D_{AB} \cdot v_m}{\pi \cdot r_m} \right)^{0,5} \quad (9)$$

where: v_m – near surface velocity of induction-stirred liquid metal,

r_m – radius of the liquid metal surface (assumed to be the melting pot inner radius),

D_{AB} – diffusion coefficient of the transfer component in the liquid phase.

In order to determine the diffusion coefficient, the following relation was used [9]:

$$D_{AB} = 10^{-8} \exp \left[\frac{250000}{R} \left(\frac{1}{1925} - \frac{1}{T} \right) \right] \quad (10)$$

Based on [10], the level of near surface velocity of induction-stirred liquid metal was assumed to be 0.135 m s^{-1} . β_{Al}^l values, estimated on this basis, are also listed in Table 4.

TABLE 4
 Aluminium mass transfer coefficients at 1973 K

Experiment no.	Overall Al mass transfer coefficient, $\text{m} \cdot \text{s}^{-1}$	Al mass transfer coefficient in the liquid phase, $\text{m} \cdot \text{s}^{-1}$
1	$1,07 \cdot 10^{-5}$	$3,34 \cdot 10^{-4}$
2	$0,97 \cdot 10^{-5}$	$3,34 \cdot 10^{-4}$
3	$1,54 \cdot 10^{-5}$	$3,34 \cdot 10^{-4}$
4	$1,50 \cdot 10^{-5}$	$3,34 \cdot 10^{-4}$
5	$1,54 \cdot 10^{-5}$	$3,34 \cdot 10^{-4}$
6	$1,75 \cdot 10^{-5}$	$3,34 \cdot 10^{-4}$
7	$1,78 \cdot 10^{-5}$	$3,34 \cdot 10^{-4}$
8	$1,82 \cdot 10^{-5}$	$3,34 \cdot 10^{-4}$
9	$1,88 \cdot 10^{-5}$	$3,34 \cdot 10^{-4}$
10	$1,93 \cdot 10^{-5}$	$3,34 \cdot 10^{-4}$

In the analysis of experimental values of mass transfer coefficient k_{Al} , a significant impact of pressure on the rate of the investigated aluminum evaporation process was demonstrated (Fig. 3). The experimental values are in a very good agreement with the results obtained by other authors who also studied the process of aluminum evaporation from titanium alloys (Table 5).

For the entire pressure range, the fraction of mass transfer resistance in the liquid phase with regard to the overall resistance of the process $\frac{k_{Al}}{\beta_{Al}^l} \cdot 100\%$ does not exceed 6% (Fig. 4) which means that the process rate is not determined by aluminum transfer in the titanium bath.

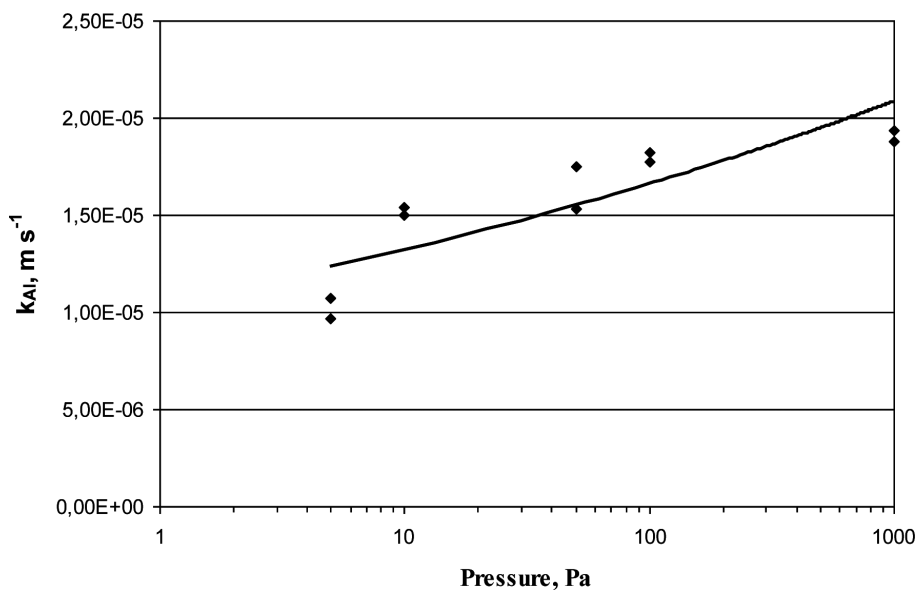


Fig. 3. Relation of the overall mass transport coefficient k_{Al} and pressure at 1973 K

TABLE 5

Overall mass transport coefficients k_{Al} determined by other authors

Technology	Alloy	Temperature range, K	Pressure range, Pa	Overall Al mass transfer coefficient, $m \cdot s^{-1}$	References
EBM	Ti-64 Ti-811	1973-2273	0,001-0,1	$2,71 \cdot 10^{-6}$ - $2,51 \cdot 10^{-5}$	[11]
EBM	Ti-6Al-4V	2223	$7 \cdot 10^{-1}$	$2,15 \cdot 10^{-5}$	[12]
VIM – skull melting*	Ti-34Al	1875-1975	1,33-133	$1 \cdot 10^{-5}$ - $3,5 \cdot 10^{-5}$	[13]
VIM	Ti-6Al-4V	1973	5-1000	$0,97 \cdot 10^{-5}$ - $1,93 \cdot 10^{-5}$	present work

* calculated on the base of mathematic modeling

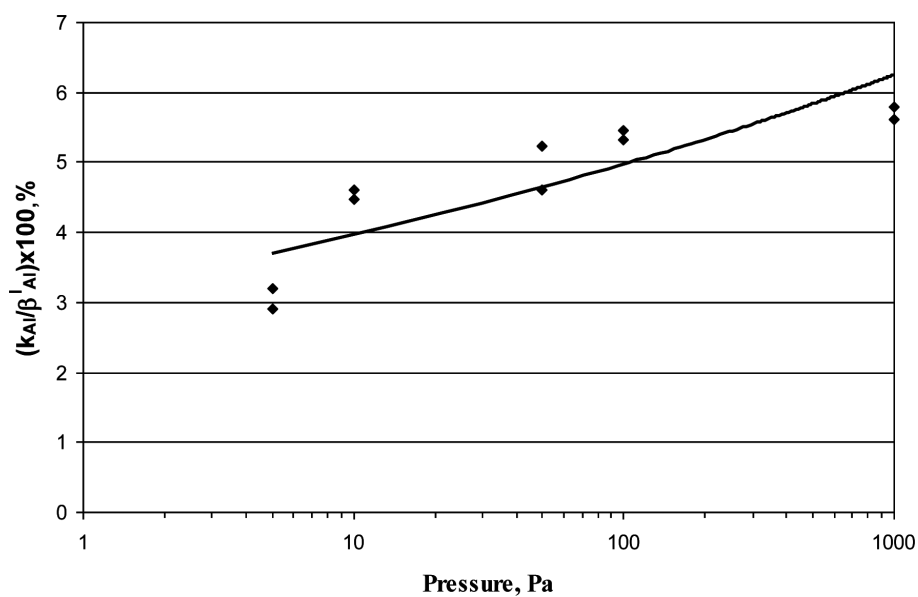


Fig. 4. Fraction of mass transfer resistance in the liquid phase with regard to the overall resistance of the process at 1973 K

5. Summary

Based on the experimental results, the kinetic analysis of aluminum evaporation from liquid Ti-6Al-4V alloys during their remelting in the VIM induction furnace yielded the following conclusions:

- ▶ Within the whole range examined, the change in aluminum concentration in titanium during remelting in a vacuum induction furnace can be described with a 1st order chemical reaction equation.
- ▶ From the kinetic point of view, it has been demonstrated that for 5 to 1000 Pa, the process of aluminum evaporation is not determined by the phenomena of mass transfer in the liquid metallic phase.
- ▶ The fraction of mass transfer resistance in the liquid phase does not exceed 6 % of the overall process resistance.

Acknowledgements

The study was conducted under the Research Project No. N N508 589439, financed by the Ministry of Science and Higher Education – Poland.

REFERENCES

- [1] L. Blach a, Untersuchungen der antimonentfernungsgeschwindigkeit aus blisterkupfer im prozess der vakuummraffination, *Archives of Metallurgy and Materials* **50** (4), 989-1002 (2005).
- [2] L. Blach a, Bleientfernung aus kupferlegierungen im prozess der vakuummraffination, *Archives of Metallurgy* **48** (1), 105-127 (2003).
- [3] J.P. Bellot, H. Duval, M. Ritchie, A. Mitchell, D. Ab litz er, Evaporation of Fe and Cr from induction-stirred austenitic stainless steel-influence of the inert gas pressure, *ISIJ International* **41** (7), 696-705 (2001).
- [4] R. Przyłucki, S. Golak, B. Oleksiak, L. Blach a, Influence of the geometry of the arrangement inductor-crucible to the velocity of the transport of mass in the liquid metallic phase mixed inductive, *Archives of Civil and Mechanical Engineering* **11** (1), 171-179 (2011).
- [5] L. Blach a, J. Łabaj, Factors determining the rate of the process of metal bath components evaporation, *Metalurgija* **51** (4), 529-533 (2012).
- [6] R. Przyłucki, S. Golak, B. Oleksiak, L. Blach a, Influence of an induction furnace's electric parameters on mass transfer velocity in the liquid phase, *Metalurgija* **51** (1), 67-70 (2012).
- [7] J. Łabaj, *Kinetyka parowania miedzi z ciekłego żelaza*, Oldprint, Katowice (2010).
- [8] F.D. Richardson, *Physical chemistry of melts in metallurgy*, Academic Press, Londyn (1974).
- [9] S.L. Semiatin, V.G. Ivanchenko, S.V. Akhonin, O.M. Ivasishin, Diffusion models for evaporation losses elektron-beam melting of alpha/beta-titanium alloys, *Metallurgical and Materials Transactions B* **35B**, 235-245 (2004).
- [10] G. Jingjie, L. Guizhong, S. Yanqing, D. Hongsheng, J. Jun, F. Hengzhi, Evaporation of multi-components in Ti-25Al-25Nb melt during induction skull melting process, *Trans. Nonferrous Met. Soc. China* **12** (4), 587-591 (2002).
- [11] T. Isawa, H. Nakamura, K. Murakami, Aluminum evaporation from titanium alloys in EB hearth melting, *ISIJ International* **32** (5), 607-615 (1992).
- [12] S. Watakabe, K. Suzuki, K. Nishikawa, Control of chemical compositions of Ti-6Al-4V alloy during melting by electron beam furnace, *ISIJ International* **32** (5), 625-629 (1992).
- [13] S. Yanqing, G. Jingjie, J. Jun, L. Guizhong, L. Yuan, Composition control of a TiAl melt during the induction skull melting (ISM) process, *Journal of Alloys and Compounds* **334**, 261-266 (2002).